CHIN. PHYS. LETT. Vol. 36, No. 10 (2019) 107102

Charge Transport Properties of the Majorana Zero Mode Induced Noncollinear Spin Selective Andreev Reflection *

Xin Shang(尚欣), Hai-Wen Liu(刘海文)**, Ke Xia(夏钶)**

Department of Physics, Beijing Normal University, Beijing 100875

(Received 7 September 2018)

We study the charge transport properties of the spin-selective Andreev reflection (SSAR) effect between a spin polarized scanning tunneling microscope (STM) tip and a Majorana zero mode (MZM). Considering both the MZM and the excited states, we calculate the conductance and the shot noise power of the noncollinear SSAR using scattering theory. We find that the excited states give rise to inside peaks. Moreover, we numerically calculate the shot noise power and the Fano factor of the SSAR effect. Our calculation shows that the shot noise power and the Fano factor are related to the angle between the spin polarization direction of the STM tip and that of the MZM, which provide additional characteristics to detect the MZM via SSAR.

PACS: 71.10.Pm, 74.45.+c, 74.78.−w, 85.75.−d DOI: 10.1088/0256-307X/36/10/107102

The Majorana zero mode (MZM) is a special type of Bogoliubov quasiparticle excitation with non-Abelian statistics, which forms the base of topological quantum computations,[1−7] and has received a large amount of research interest since being proposed. There are a number of methods that have been used to generate and detect the MZM in condensed matter systems,[5,7−9] these include a chiral p-wave superconductor,[10] the $\nu = 5/2$ fractional quantum Hall system,[1,2] topological insulator (TI)/s-wave superconductor (SC) interfaces with the MZM in the vortex core,[11] proximity-induced superconductors for spin-orbit coupled nanowires,[6,12] and a triple-quantum dot system.[13] An electron with its spin direction aligned with the MZM will undergo an Andreev reflection, while an electron with opposite spin direction will not.[14−18] This allows us to detect the existence of the MZM using ferromagnetic STM.[14−18]

However, previous studies of 2D SSAR have only the collinear spin transport, for example, the spin polarization of the lead being parallel or antiparallel to that of the MZM. The excited states, which have low energy above the MZM, were ignored.[18] To obtain more information concerning SSAR, we consider both the MZM and the excited states in the SSAR effect when the spin polarization direction of the STM tip and the MZM are noncollinear. In addition, compared to the conductance, the shot noise may shed more light on the underlying physical properties of the system.[19] In particular, the shot noise can be used to determine the charge and statistics of the quasiparticles relevant to transport, and to reveal information concerning the potential and internal energy scales of mesoscopic systems.[19] In this study, we calculate the shot noise power and the Fano factor of the SSAR to provide additional approaches to detect the MZM using SSAR.

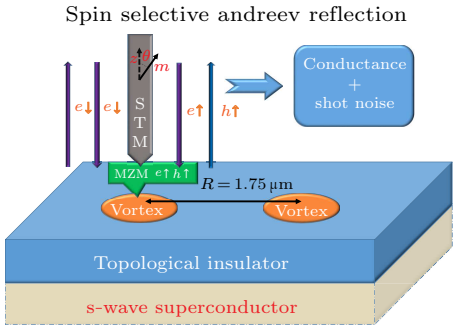

Fig. 1. The Majorana induced spin selective Andreev reflection. An MZM exists in the vortex core of a 3D TI, which is under an s-wave superconductor. An electron with the same spin as the MZM will undergo an Andreev reflection, whereas an electron with an opposite spin direction will not. The conductance and the shot noise power of this SSAR induced current may be related to the spin polarization of the STM tip.

As shown in Fig. 1, we consider a TI covered by a superconductor. Superconductivity is induced in the TI via the proximity effect, and a vortex state is formed in the surface of the TI under a magnetic field. At the center of the vortex core ($r = 0$), the spin polarization of the MZM is parallel to the magnetic field.

Let us construct the Hamiltonian of the vortex state in a topological superconductor (TS). This TS is modeled by a helical surface state with Rashba spin-orbit coupling and proximity-induced superconductivity.[18] The helical surface state is the surface state of a 3D TI in the x–y plane. We can generalize the Hamiltonian in the x–y plane to a spherical

*Supported by the National Natural Science Foundation of China under Grant Nos 11674028, 61774017, 11734004 and 21421003, and the National Key Research and Development Program of China under Grant No 2017YFA0303300.

**Corresponding author. Email: haiwen.liu@bnu.edu.cn; kexia@bnu.edu.cn

© 2019 Chinese Physical Society and IOP Publishing Ltd

surface of radius R.

The Hamiltonian of the vortex state can be written as

$$H_\nu = \begin{bmatrix} H_{0\mathrm{e}} & \Delta \\ \Delta^* & H_{0\mathrm{h}} \end{bmatrix}, \tag{1}$$

where $H_{0\mathrm{e(h)}}$ is the single-electron (hole) Hamiltonian of a helical surface state, and Δ is the proximity-induced superconducting order parameter, and the superscript $*$ represents the conjugation. The single-electron Hamiltonian of a helical surface state[18] is

$$H_{0\mathrm{e}} = -\frac{\alpha}{R\hbar}\hat{L}\times\hat{\sigma} - \mu, \tag{2}$$

where α is the spin-orbit coupling strength, $\hat{\sigma}$ represents the Pauli matrices, $\hat{L}$ is the orbital angular momentum, and μ is the chemical potential. The single-hole Hamiltonian $H_{0\mathrm{h}}$ is defined as $-\sigma_y H_{0\mathrm{e}}\sigma_y^*$ with σ_y^* being a conjugated Pauli matrix.

The vortex state can be described as $\Delta = \Delta(\theta)e^{i\phi}$. Here the factor $e^{i\phi}$ describes a vortex with a winding number of 1 and $\Delta(\theta) = \Delta_0\tanh(\frac{R\sin\theta}{\xi_0})$ with ξ_0 characterizing the size of the vortex core. For details of how to obtain zero mode, the first and second excited states, one can see the Supplementary Material.

Next, let us consider the total Hamiltonian of a system with a vortex state coupling to a spin polarization STM tip.

The Hamiltonian of the STM tip is

$$H_L = \begin{bmatrix} H_{L,e} & 0 \\ 0 & H_{L,h} \end{bmatrix}, \tag{3}$$

where $H_{L,e}$ ($H_{L,h}$ defined as $-\sigma_y H_{L,e}\sigma_y^*$) is the Hamiltonian of the electron (hole) on the STM tip. The Hamiltonian of the electron on the STM tip can be described as[20]

$$H_{L,e} = \sum\nolimits_\sigma \hat{d}^+_{L,\sigma}(\varepsilon_\sigma - \mu_L + \hat{\sigma}\cdot\hat{M})\hat{d}_{L,\sigma}, \tag{4}$$

where $\hat{d}^{(+)}_{L,\sigma}$ denotes the electron annihilation (creation) operator of the STM tip with σ spin, μ_L indicates the chemical potential of the STM tip (set to zero), ε_σ is the kinetic energy of the STM tip with σ spin, $\hat{M}$ is the spin related potential, and $\hat{\sigma}$ are Pauli matrices. The coupling between the vortex states and the STM tip can be described using the following Hamiltonian[20]

$$H_{\nu-L} = \sum\nolimits_{n,\sigma}\Big\{2t_{n\sigma}\Big(\cos\frac{\theta}{2}\hat{d}^+_{L,\sigma} - \sigma\cdot\sin\frac{\theta}{2}\hat{d}^+_{L,\bar{\sigma}}\Big)\hat{c}_{n,\sigma} + \mathrm{c.c.}\Big\}, \tag{5}$$

where $t_{n\sigma}$ is the coupling strength between the vortex and the STM tip. The retarded Green's function of the system can be obtained via Dyson's equation

$$G^{\mathrm{tot}} = \frac{1}{(G^{0,\mathrm{R}})^{-1} - \Sigma^r}, \tag{6}$$

where the single-particle retarded Green's function $G^{0,\mathrm{R}}$ can be constructed with the wave functions $\hat{\Psi}_m$ and the eigenvalue E_m of the vortex state. The self-energy $\Sigma^r = H_{v-L}\lambda^r H_{L-v}$ with $\lambda^r = \sum_m \frac{|\phi^1_m\rangle\langle\phi^1_m|}{E-E_m+i\delta}$ is the single-particle retarded Green's function of the STM tip, E_m is the eigenvalue of H_L, $|\phi^1_m\rangle$ is the eigenfunction of H_L, and δ is a positive infinitesimal.[20]

The S matrix can be obtained via the Fisher–Lee formula[21]

$$S = \begin{bmatrix} r_{\mathrm{ee}} & r_{\mathrm{eh}} \\ r_{\mathrm{he}} & r_{\mathrm{hh}} \end{bmatrix} = -I + i\Gamma^{1/2}\times G^{\mathrm{tot}}\times\Gamma^{1/2}, \tag{7}$$

where Γ is the broadening function defined as $\Gamma = i(\Sigma^r - \Sigma^{r+})$, $r_{\mathrm{ee(hh)}}$ is a 2×2 matrix describing the probability of an electron (hole) being reflected as an electron (hole), while $r_{\mathrm{eh(he)}}$ is a 2×2 matrix describing the probability of an electron (hole) being reflected as a hole (electron) in spin space. The current I_c can be defined as

$$I_\mathrm{c} = \frac{e}{h}\int_0^\infty [\langle a^+_\mathrm{e}(E)a_\mathrm{e}(E)\rangle - \langle b^+_\mathrm{e}(E)b_\mathrm{e}(E)\rangle - \langle a^+_\mathrm{h}(E)a_\mathrm{h}(E)\rangle + \langle b^+_\mathrm{h}(E)b_\mathrm{h}(E)\rangle]dE, \tag{8}$$

where $a^{+(-)}_{\mathrm{e(h)}}(E)$ is the generate (annihilation) operator of an incoming electron (hole), $b^{+(-)}_{\mathrm{e(h)}}(E)$ is the generate (annihilation) operator of a outgoing electron (hole). The differential conductance can also be obtained.[22]

The shot noise includes additional information concerning the fluctuation and can be calculated by[19]

$$P_\mathrm{s}(t-t') = \frac{1}{2}\langle\Delta I_L(t)\Delta I_L(t') + \Delta I_L(t')\Delta I_L(t)\rangle, \tag{9}$$

where $\Delta I_L(t) = I_L(t) - I_{L0}$, and I_{L0} is the average of $I_L(t)$. The Fano factor[18] is defined as

$$F = \frac{P_\mathrm{s}}{2eI}. \tag{10}$$

Both the shot noise power P_s and the Fano factor F can be obtained from the S-matrix.

Then, we calculate the charge transport properties of SSAR when STM tip contact with the point, which is 1 nm away from the vortex core (the results of the vortex core are shown in the Supplementary Material, which are consistent with the previous studies[14]).

As shown in Fig. 2, when $\theta = 0°$, the conductance line has one broad peak with a maximum value of two at zero energy. Moreover, there are four sharp peaks near the energy of the first and second excited states. Then, with the decrease of θ, the width of the broad peak is much smaller. Therefore, the influence of the excited states decreases as θ increases.

To determine the influence of the first excited states, we calculate the conductance with different θ

for two cases. In the first case, we ignore the first excited states, and in the second case, we consider the first excited states.

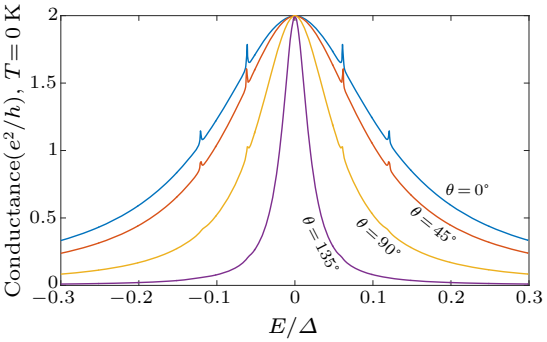

Fig. 2. The angular dependence of the conductance in the SSAR effect. The experimental data of the tunneling conductance consists of two parts, the first term is the contribution from the normal tunneling and the second term from the Andreev reflection.[17] Our results focus on the Andreev reflection part. The maximum value of the conductance at zero energy is 2. This value is the same as two times the ratio of the electron spin projected in the direction of MZM spin polarization. In addition, when θ is small, there are four more peaks in the conductance line. These two peaks may be due to the contribution of the excited states.

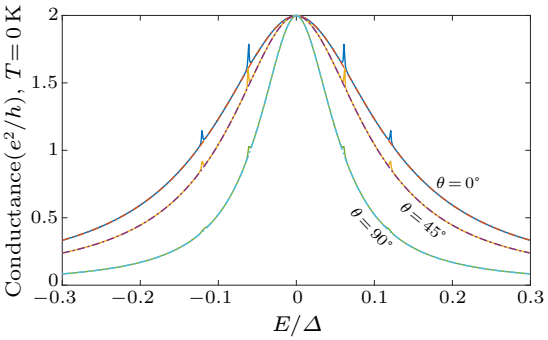

Fig. 3. The conductance when considering the first and second excited states (solid line) or not (dotted line). The excited states can induce four more peaks near the energy of the first and the second excited states. These two conductances become similar when $\theta > 90°$.

From Fig. 3, we can see that the excited states can induce four more peaks on conductance of the SSAR when $\theta = 0°$. However, under the noncollinear condition, the excited states have several novel features with different θ. When θ is small, the first and second excited states can induce additional peaks at the energy of them, while the excited states cannot induce them in the case of large θ. The different properties between the two conditions can be explained using Green's function of the system (see the Supplementary Material).

The above analysis is performed in the case of zero temperature. Here we study the transport properties under finite temperature conditions in a specific case with $\theta = 0°$. As shown in Fig. 4, the conductance decreases greatly with increasing temperature, while the width of the conductance increases with the temperature. Due to the thermal broadening under finite temperature, the width of the conductance increases while the maximum value of the conductance decreases.

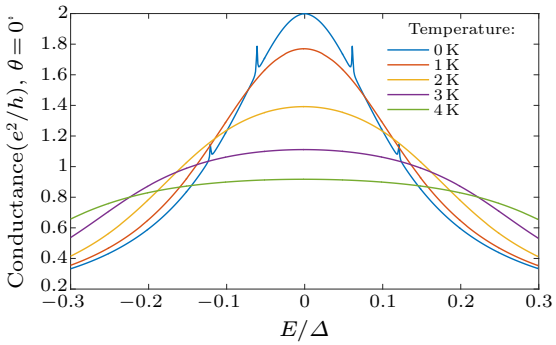

Fig. 4. The temperature dependence of the conductance in the SSAR effect when $\theta = 0°$. With increasing temperature, the conductance at zero energy is greatly decreased and the width of the conductance line increases.

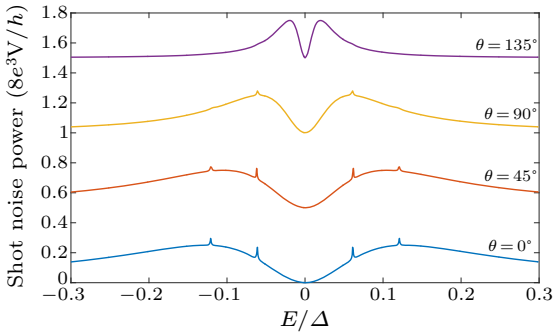

Fig. 5. The angular dependence of the shot noise power, When $\theta = 0°$, 45°, 90° and 135°, there are shifts of, 0.5, 1 and 1.5. The shot noise power forms a valley near the zero energy with some peaks near some energies of excited states. Moreover, the shot noise power at zero energy is zero. In addition, the width of the valley is smaller with increasing θ.

At zero energy, as shown in Fig. 5, we find that the shot noise is zero due to the full reflection of the electrons. Let us focus on the formula of the shot noise power. As mentioned above, all of the spin-up electrons can be reflected as holes with the same spin while the spin-down electron can be reflected as themselves at zero temperature. The term that contains $(r^{+}_{\mathrm{eh(he)}}a^{+}_{\mathrm{h(e)}}(E)r_{\mathrm{hh(ee)}}a_{\mathrm{h(e)}}(E))$ should be zero at zero temperature. Therefore, the shot noise power can be simplified to $P_{\mathrm{s}} = \frac{2e^3V}{h}[(r^{+}_{\mathrm{he}}a^{+}_{\mathrm{e}}(E)r_{\mathrm{he}}a_{\mathrm{e}}(E))(r^{+}_{\mathrm{hh}}a^{+}_{\mathrm{h}}(E)r_{\mathrm{hh}}a_{\mathrm{h}}(E)) + (r^{+}_{\mathrm{ee}}a^{+}_{\mathrm{e}}(E)r_{\mathrm{ee}}a_{\mathrm{e}}(E))(r^{+}_{\mathrm{eh}}a^{+}_{\mathrm{h}}(E)r_{\mathrm{eh}}a_{\mathrm{h}}(E))]$. In other words, the shot noise power is proportional to the probability of an electron being reflected as a hole times the probability of an electron being reflected as itself at zero energy.

Now, let us look at the shot noise power non-zero energy. We find that, in the collinear case with increasing the absolute energy, the shot noise power is firstly increases and then decreases to form a major valley. Furthermore, the shot noise powers have some peaks near the energy of excited states. In addition,

the width of the valley is decreased with the increase of θ.

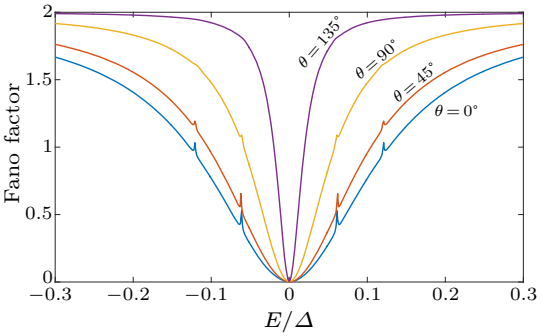

Fig. 6. The angular dependence of the Fano factor in the SSAR effect. As opposed to normal Andreev reflection, the Fano factor at zero energy is zero.

As shown in Fig. 6, the Fano factor is similar to two minus the value of the conductance. The Fano factor almost always increases with the absolute energy which forms a wide valley near the zero energy with some peaks near the energy of excited states. Moreover, the Fano factor is always zero at zero energy, which is very different from normal Andreev reflection,[23–25] where the Fano factor equals two.[19] This can be explained by the probability of an electron being reflected as a hole. The Fano factor is proportional to the probability that an electron is reflected as itself. This probability always increases from 1 to 0 with increasing the absolute energy. Moreover, as mentioned above, the first excited states will influence the probability that an electron is reflected as a hole. This means that the first excited states also have an influence on the shot noise power and the Fano factor. In more detail, the excited states can cause more peaks due to the new peak of the conductance induced by the excited states.

In summary, we have built a model to study the charge transport properties of the SSAR effect. Considering both the MZM and the excited states, we have studied the conductance and the shot noise of the SSAR effect using Green's function combined with scattering theory. Firstly, we numerically calculate the angular dependence of the conductance in the SSAR effect. It is found that the excited states can increase the conductance at zero energy. Then, we calculate the influence of the temperature under finite temperature conditions. With increasing temperature, the maximum of conductance decreases, while the width of conductance increases. At low temperatures, the influence of the excited states is also obvious. Finally, we study the shot noise power and the Fano factor of the SSAR effect. We find that, at zero energy, the shot noise power is zero, meanwhile, the Fano factor is also zero. This is very different from normal Andreev reflection where the Fano factor is two.[19] In addition, the shot noise power is also influenced by the excited states of the vortex state. These transport properties can provide more information concerning the detection of MZM via the SSAR effect.

References

[1] Moore G and Read N 1991 *Nucl. Phys. B* **360** 362
[2] Read N and Green D 2000 *Phys. Rev. B* **61** 10267
[3] Kitaev A Y 2001 *Phys.-Usp.* **44** 131
[4] Kitaev A Y 2003 *Ann. Phys.* **303** 2
[5] Nayak C, Simon S H, Stern A, Freedman M and Sarma S D 2008 *Rev. Mod. Phys.* **80** 1083
[6] Oreg Y, Refael G and von Oppen F 2010 *Phys. Rev. Lett.* **105** 177002
[7] Elliott S R and Franz M 2015 *Rev. Mod. Phys.* **87** 137
[8] Zhu G Y, Wang R R, Zhang G M 2017 *Physics* **46** 154 (in Chinese)
[9] Aguado R 2017 *Riv. Nuovo Cimento* **40** 523
[10] Sarma S D, Nayak C and Tewari S 2006 *Phys. Rev. B* **73** 220502
[11] Fu L and Kane C L 2008 *Phys. Rev. Lett.* **100** 096407
[12] Lutchyn R M, Sau J D and Sarma D S 2010 *Phys. Rev. Lett.* **105** 077001
[13] Deng M X, Zheng S H, Yang M, Hu L B and Wang R Q 2015 *Chin. Phys. B* **24** 037302
[14] He J J, Ng T K, Lee P A and Law K T 2014 *Phys. Rev. Lett.* **112** 037001
[15] Xu J P, Liu C, Wang M X, Ge J, Liu Z L, Yang X, Chen Y, Liu Y, Xu Z A, Gao C L, Qian D, Zhang F C and Jia J F 2014 *Phys. Rev. Lett.* **112** 217001
[16] Kawakami T and Hu X 2015 *Phys. Rev. Lett.* **115** 177001
[17] Sun H H, Zhang K W, Hu L H, Li C, Wang G Y, Ma H Y, Xu Z A, Gao C L, Guan D D, Li Y Y, Liu C, Qian D, Zhou Y, Fu L, Li S C, Zhang F C and Jia J F 2016 *Phys. Rev. Lett.* **116** 257003
[18] Hu L H, Li C, Xu D H, Zhou Y and Zhang F C 2016 *Phys. Rev. B* **94** 224501
[19] Blanter Y and Bttiker M 2000 *Phys. Rep.* **336** 1
[20] Sergueev N, Sun Q F, Guo H, Wang B and Wang J 2002 *Phys. Rev. B* **65** 165303
[21] Fisher D S and Lee P A 1981 *Phys. Rev. B* **23** 6851
[22] Datta S 1997 *Electronic Transport in Mesoscopic Systems, Cambridge Studies in Semiconductor Physics, Microelectronic Engineering* (Cambridge: Cambridge University Press)
[23] Klapwijk T, Blonder G and Tinkham M 1982 *Physica B+C* **109–110** 1657
[24] Kashiwaya S and Tanaka Y 2000 *Rep. Prog. Phys.* **63** 1641
[25] Tinkham M 2004 *Introduction to Superconductivity* 2nd edn (Dover: Courier Corporation)

Supplementary Material: Charge transport properties of the Majorana zero mode induced noncollinear spin selective Andreev reflection*

Xin Shang(尚欣), Hai-Wen Liu(刘海文)*, Ke Xia(夏钶)**,

Department of Physics, Beijing Normal University, Beijing 100875

*Supported by the National Natural Science Foundation of China (No.11674028, No.61774017, No.11734004 and No.21421003) and National Key Research and Development Program of China (Grant No. 2017YFA0303300).

*haiwen.liu@bnu.edu.cn

** kexia@bnu.edu.cn

%Email: 201531140007@mail.bnu.edu.cn

Text A: Theoretical Model

As shown in Figure S1, we consider a topological insulator (TI) covered by a superconductor. Superconductivity is induced in the TI via the proximity effect, and a vortex state is formed in the surface of the TI under a magnetic field. At the center of the vortex core(r = 0), the spin polarization of the MZM is parallel to the magnetic field.

Let us construct the Hamiltonian of the vortex state in a topological superconductor (TS). This TS is modeled by a helical surface state with Rashba spin--orbit coupling and proximity-induced superconductivity [S1]. The helical surface state is the surface state of a 3D topological insulator in the x--y plane. We can generalize the Hamiltonian in the x--y plane to a spherical surface of radius R.

The single-electron Hamiltonian of a helical surface state is [S1]:

$$H_{0e} = -\frac{\alpha}{R\hbar}\hat{L} \times \hat{\sigma} - \mu, \tag{s1}$$

where α is the spin-orbit coupling strength, $\hat{\sigma}$ is the Pauli matrices, $\hat{L}$ are the orbital angular momentum, and μ is the chemical potential. The single-hole Hamiltonian (H_{0h}) defined as -$\sigma_y H_{0e}\sigma_y^*$ and σ_y is a pauli matrix.

The Hamiltonian of the proximity-induced superconducting state can be described as:

$$H_\Delta = \Delta(c_\downarrow c_\uparrow - c_\uparrow c_\downarrow) + \Delta^*(c_\downarrow^+ c_\uparrow^+ - c_\uparrow^+ c_\downarrow^+), \tag{s2}$$

where Δ is the proximity induced superconducting order parameter ans $c_\sigma^{(+)}$ is the electron annihilation (creation) operator with $\sigma = \uparrow\downarrow$ denoting the spin.

Then, in the standard Nambu representation, the field operator can be defined as

$$\hat{\psi}(r) = [\hat{c}_\uparrow, \hat{c}_\downarrow, \hat{c}_\downarrow^+, -\hat{c}_\uparrow^+]^T. \tag{s3}$$

The Hamiltonian of the proximity-induced superconducting state in then

$$H_\Delta = \begin{bmatrix} 0 & \Delta I \\ \Delta^* I & 0 \end{bmatrix}, \tag{s4}$$

where *I* is the unit matrix.

The Hamiltonian of the vortex state can be written as:

$$H_v = \begin{bmatrix} H_{0e} & \Delta I \\ \Delta^* & H_{0h} \end{bmatrix}, \tag{s5}$$

where H_{0h} is the single-hole Hamiltonian of a helical surface state defined as -$\sigma_y H_{0e}\sigma_y^*$ and σ_y is a pauli matrix.

The vortex state can be described as $\Delta = \Delta(\theta)e^{i\phi}$. Here the factor $e^{i\phi}$ describes a vortex with a winding number of 1 and $\Delta(\theta) = \Delta_0 tanh(\frac{Rsin\theta}{\xi_0})$, where ξ_0 characterizes the size of the vortex core.

By diagonalzingH_v, we can define a new quantum number of K_z [S1], where$K_z|\Phi_m> = m|\Phi_m>$, where m and $|\Phi_m>$ are the eigenvalue and eigenfunction of K_z. Here $K_z = l_z + \sigma_z + \tau_z$ is the orbital quantum number in the z direction, σ_z is the spin quantum number in the z direction, τ_z is

the spin-orbit-pseudospin quantum number referring to the particle-hole degree of freedom and $|\Phi_m>$ is the four-component wave function [S1].

$$|\Phi_m>=[e^{im\phi}u_1, e^{i(m+1)\phi}u_2, e^{i(m-1)\phi}v_1, e^{im\phi}v_2] \quad \text{(s6)}$$

The eigenvalue problem then becomes

$$H_v|\Phi_m>=E_m|\Phi_m>. \quad \text{(s7)}$$

The four-component eigenfunction basis [S1-S2] in $|\Phi_m>$ can be expressed in terms of the spherical harmonic functions: $e^{im\phi}u_1=\sum_l a_l Y_l^m$, $e^{i(m+1)\phi}u_2=\sum_l b_l Y_l^{m+1}$, $e^{i(m-1)\phi}v_1=\sum_l c_l Y_l^{m-1}$, $e^{im\phi}v_2=\sum_l d_l Y_l^m$, where $Y_l^m(\theta,\phi)=P_l^m(cos\theta)e^{im\phi}/\sqrt{2\phi}$ and $P_l^m(cos\theta)$ is the associated Legendre polynomial.

By directly diagonalizing the H_v, we can obtain the wave function and the energy spectrum. In our numerical calculations, we set $R=50\xi_0$, α=30 meV·nm, ξ_0=35 nm, Δ_0=1 meV, and μ =90 meV, which are comparable to the experiment data in Bi_2Se_3[S3]. Taking a cutoff in the orbital angular momentum l to be approximately 200, we find that for m = zero, E_0 = zero (numerically $\pm 4\times 10^{-6}$ meV). Here u_1=v_2 ≠0, and u_2=$v_1=0$; this means that a spin up electron and a spin up hole occupy the MZM. For the m=1 state, E_{-1}=-0.06 meV, v_1 ≠0, u_2=0, u_1=0 and v_2=0; only a hole with a down spin can occupy this state. Meanwhile, for m=-1, E_1=0.06$ meV, $u_2\neq 0$, u_1, v_1 and v_2=0, only a spin down electron can occupy this state. These are the first excited states of the vortex. When |m|>1, v_1, u_2, u_1,and v_2 are equal to zero at the core of the vortex.

Next, let us consider the total Hamiltonian of a system with a vortex state coupling to a spin polarization STM tip. The Hamiltonian of the electron on the STM tip can be described as[S4]:

$$H_{L,e}=\sum_\sigma \hat{d}_{L,\sigma}^{+}(\varepsilon_\sigma-\mu_L+\sigma M)\hat{d}_{L,\sigma} \quad \text{(s8)}$$

where $\hat{d}_{L,\sigma}^{+}$ denotes the electron annihilation (creation) operator of the STM tip with σ spin, μ_L indicates the chemical potential of the STM tip (set to zero), ε_σ is the kinetic energy of the STM tip with σ spin, $\hat{M}$ is the spin related potential and $\hat{\sigma}$ are Pauli matrices.

The Hamiltonian of the STM tip is

$$H_L=\begin{bmatrix} H_{L,e} & 0 \\ 0 & H_{L,h} \end{bmatrix}, \quad \text{(s9)}$$

where ($H_{L,h}$) defined as -$\sigma_y H_{L,e}\sigma_y^*$ is the Hamiltonian of the electron(hole) on the STM tip.

The coupling between the vortex states and the STM tip can be described using the following Hamiltonian [S4]:

$$H_{L-v} = \sum_{n,\sigma}\{2t_{n\sigma}(cos\frac{\theta}{2}\hat{d}^{+}_{L,\sigma} - \sigma \cdot sin\frac{\theta}{2}\hat{d}^{+}_{L,\bar{\sigma}})\hat{c}_{n,\sigma} + H.c.\}, \qquad \text{(s10)}$$

where t_c is the coupling strength between the vortex and the STM tip.

The total Hamiltonian of the system is:

$$H_{tot} = \begin{bmatrix} H_L & H_{L-v} \\ H_{v-L} & H_v \end{bmatrix}. \qquad \text{(s11)}$$

The retarded Green's function of the system can be obtained via Dyson's equation:

$$G^{tot} = \frac{1}{(G^{0,R})^{-1} - \Sigma^r}. \qquad \text{(s12)}$$

Here, the single-particle retarded Green's function $G^{0,R}$ can be constructed with the wave functions $\hat{\Psi}_m$ and the eigenvalue E_m of the vortex state:

$$G^{0,R} = \sum_m \frac{|\hat{\Psi}_m><\hat{\Psi}_m|}{E - E_m + i\delta}, \qquad \text{(s13)}$$

Where $|\hat{\Psi}_m >= [e^{im\phi}u_1, e^{i(m+1)\phi}u_2, e^{im\phi}v_2, e^{i(m-1)\phi}v_1]$ and $\delta\ is$ a positive infinitesimal.

We assume that the spin polarization of the FM tip $\widehat{M}$ has an angle θ with respect to the z direction(the direction of the MZM spin polarization).

The self-energy $\Sigma^r = H_{v-L}\lambda^r H_{L-v}$ with $\lambda^r = \sum_m \frac{|\phi^1_m><\phi^1_m|}{E - E_m + i\delta}$ is the single-particle retarded Green's function of the STM tip. E_m is the eigenvalue of H_L and $|\phi^1_m >$ is the eigenfunction of H_L, $\delta\ is$ a positive infinitesimal.

Then, the general form of λ^r is:

$$\lambda^r = \begin{bmatrix} \lambda_{e\uparrow\uparrow} & \lambda_{e\uparrow\downarrow} & 0 & 0 \\ \lambda_{e\downarrow\uparrow} & \lambda_{e\downarrow\downarrow} & 0 & 0 \\ 0 & 0 & \lambda_{h\uparrow\uparrow} & \lambda_{h\uparrow\downarrow} \\ 0 & 0 & \lambda_{h\downarrow\uparrow} & \lambda_{h\downarrow\downarrow} \end{bmatrix}, \qquad \text{(s14)}$$

where $\lambda_{e\uparrow\uparrow,\mathrm{nn}} = t^2_{en,\uparrow}cos^2\frac{\theta}{2}\lambda_1 + t^2_{en,\uparrow}sin^2\frac{\theta}{2}\lambda_2$, $\lambda_{e\uparrow\downarrow,\mathrm{nn}} = t_{en\uparrow}t_{en\downarrow}cos\frac{\theta}{2}sin\frac{\theta}{2}(\lambda_1 - \lambda_2)$, $\lambda_{e\downarrow\uparrow,\mathrm{nn}} = t_{en\uparrow}t_{en\downarrow}cos\frac{\theta}{2}sin\frac{\theta}{2}(\lambda_1 - \lambda_2)$, $\lambda_{e\downarrow\downarrow,\mathrm{nn}} = t^2_{en,\downarrow}cos^2\frac{\theta}{2}\lambda_1 + t^2_{en,\downarrow}sin^2\frac{\theta}{2}\lambda_2$, $\lambda_{h\uparrow\uparrow,\mathrm{nn}} = t^2_{hn,\uparrow}cos^2\frac{\theta}{2}\lambda_3 +$

$t_{hn,\uparrow}^2 sin^2\frac{\theta}{2}\lambda_4$, $\lambda_{h\uparrow\downarrow,\mathrm{nn}} = t_{hn,\uparrow}t_{hn,\downarrow}cos\frac{\theta}{2}sin\frac{\theta}{2}(\lambda_3-\lambda_4)$, $\lambda_{h\downarrow\uparrow,nn} = t_{hn,\uparrow}t_{hn,\downarrow}cos\frac{\theta}{2}sin\frac{\theta}{2}(\lambda_3-\lambda_4)$,

$\lambda_{h\downarrow\downarrow,\mathrm{nn}} = t_{hn,\downarrow}^2 cos^2\frac{\theta}{2}\lambda_3 + t_{hn,\downarrow}^2 sin^2\frac{\theta}{2}\lambda_4$, with $\lambda_1 = (E-(e_0+M)+i\delta)^{-1}$, $\lambda_2 = (E-(e_0-M)+i\delta)^{-1}$, $\lambda_3 = (E+(e_0+M)+i\delta)^{-1}$, $\lambda_4 = (E+(e_0-M)+i\delta)^{-1}$, n denote the state of vortex.Here, we use the parameter as: e=10Δ, $|M|$=7Δ,$t_{e0,\uparrow} = t_{h0,\uparrow} = t_{e1(2),\downarrow} = t_{h-1(-2),\downarrow} = 0.7\Delta$, $t_{e1(2),\uparrow} = t_{h-1(-2),\uparrow} = t_{e0,\downarrow} = t_{h0,\downarrow} = 0.2t_{e0,\uparrow}$.

The S matrix can be obtained via the Fisher-Lee formula [S5]:

$$\mathrm{S} = \begin{bmatrix} r_{ee} & r_{eh} \\ r_{he} & r_{hh} \end{bmatrix} = -I + i\Gamma^{\frac{1}{2}} \times G^{tot} \times \Gamma^{\frac{1}{2}}, \tag{s15}$$

where, Γ is the broadening function, which is defined as $\Gamma = i(\Sigma^r - \Sigma^{r+})$, $r_{ee(hh)}$ is a 2× 2 matrix describing the probability of a electron(hole) being reflected as a electron(hole), while $r_{eh(he)}$ is a 2× 2 matrix describing the probability of a electron(hole) being reflected as a hole(electron) in spin space. The current I_c can be defined as:

$$I_c = \frac{e}{h}\int_0^\infty [< a_e^+(E)a_e(E) > - < b_e^+(E)b_e(E) > - < a_h^+(E)a_h(E) > + < b_h^+(E)b_h(E) >]dE, \tag{s16}$$

where $a_{e(h)}^{+(-)}(E)$ is the generate (annihilation) operator of an incoming electron(hole), $b_{e(h)}^{+(-)}(E)$is the generate (annihilation) operator of a outgoing electron(hole). The differential conductance can also be obtained [S6].

The shot noise includes additional information concerning the fluctuation and can be calculated as [S7]

$$Sp(t-t') = \frac{1}{2} < \Delta I_L(t)\Delta I_L(t') + \Delta I_L(t')\Delta I_L(t) > \tag{s17}$$

Where $\Delta I_L(t) = I_L(t) - I_{L0}$ and I_{L0} is the average of $I_L(t)$

The shot noise under the zero temperature limit can be obtained as follows

When eV>0,

$$Sp1 = \frac{2e^3V}{h}[\left(r_{he}^{+}a_e^{+}(E)r_{he}a_e(E)\right)\left(r_{hh}^{+}a_h^{+}(E)r_{hh}a_h(E)\right) +$$

$$\left(r_{ee}^{+}a_e^{+}(E)r_{ee}a_e(E)\right)\left(r_{eh}^{+}a_h^{+}(E)r_{eh}a_h(E)\right) - \left(r_{ee}^{+}a_e^{+}(E)r_{he}a_e(E)\right)\left(r_{hh}^{+}a_h^{+}(E)r_{eh}a_h(E)\right) -$$

$$\left(r_{he}^{+}a_e^{+}(E)r_{ee}a_e(E)\right)\left(r_{eh}^{+}a_h^{+}(E)r_{hh}a_h(E)\right)] \quad \text{(s18)}$$

When eV<0, $a_e^{(+)}$ should change to $a_h^{(+)}$ and $r_{e(h)e(h)}^{(+)}$ should change to $r_{h(e)h(e)}^{(+)}$. This is because the carrier of the charge current is the change from electron to hole. When eV=0, the shot noise power should be $\frac{(Sp1(eV>0)+Sp1(ev<0))}{2}$.In other words, the shot noise power is 0 at zero temperature.

The shot noise power [6] can be simplified as *Sp:*

$$Sp = \frac{8e^3V}{h}r_{eh}^{+}r_{eh}r_{ee}^{+}r_{ee}. \quad \text{(s19)}$$

The Fano factor [6] is defined as

$$F = \frac{Sp}{2eI}. \quad \text{(s20)}$$

Both the shot noise power and the Fano factor can be obtained from the S-matrix.

Text B: Charge transport properties of SSAR when STM tip contact with the vortex core

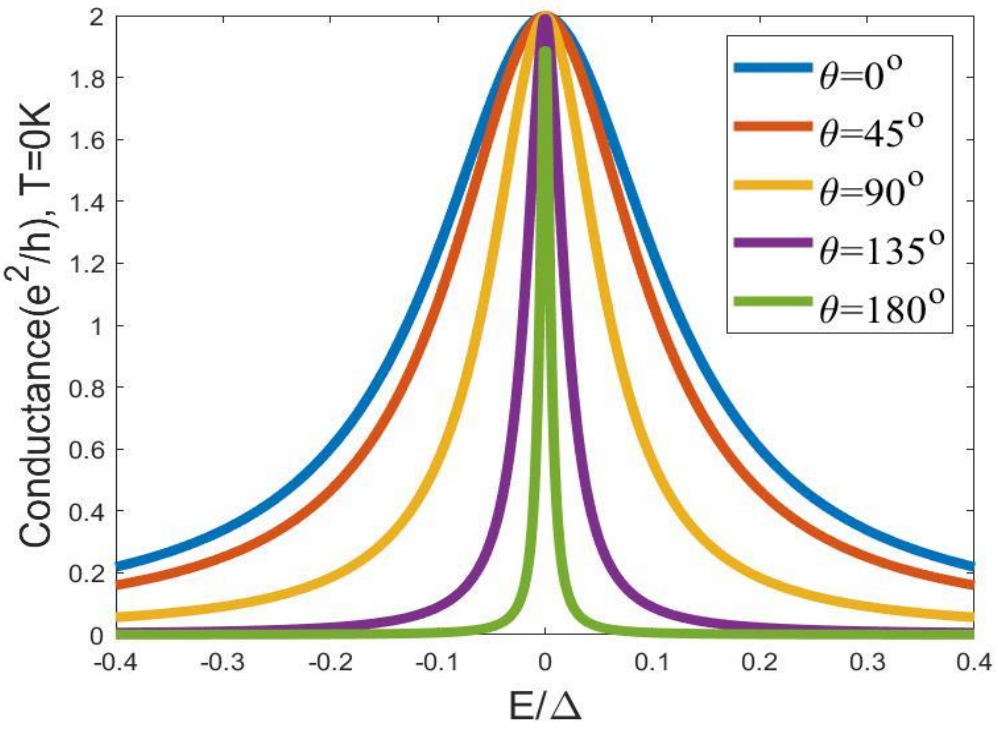

Fig. S1. The angular dependence of the conductance in the SSAR effect when STM tip contact with the vortex core. The conductance forms a peak with a maximum value of two and the width decreases with the increase of the angle, which is consistent with the previous studies [S8].

Text C: Influence of the first and second excited states on conductance

The different properties between the two conditions can be explained using the Green's function of system. From the wave function of the vortex states, we find that only the first term (u_1 for the spin-up electron, $e_\uparrow$ and the third term (v_2 for the spin-up hole, $h_\uparrow$) of the wave function($|\Psi_0>$) have non-zero values at the central of vortex when m = 0. When m = 1, only the fourth term (for the spin-down hole, $h_\downarrow$) of the wave function ($|\Psi_{-1}>$) has a non-zero value, while for m = -1, only the second term (for the spin-down electron, $e_\downarrow$) of the wave function ($|\Psi_1>$) has a non-zero value central of vortex. This means that the MZM is only local at the spin up channel of the hole and the electron, while the two first excited states are local at the spin-down channels of the electron and the hole, respectively. In the collinear case, the self-energy is a diagonal matrix and there is no coupling between the two spin channels. Only the coupling between the electron and the hole is local at the spin-up channel of the MZM.

However, in case of STM tip is contact with non-central area, the wave function of MZM have a little spin ↓ component. While the excited states have both of electron and hole component.

For example, the m=1 state，expect the spin-down hole, $h_\downarrow$, there are little component of spin up electron and spin up hole. Therefore, the excited states can contribute to the conductance in the non-central case. In this case, the excited states have two influence on the conductance, the first is more peaks at the energy of the excited states, second is decrease the conductance near the zero energy.

Here, we use the $t_{e(h),n,\uparrow(\downarrow)}$ to describe the coupling between the STM tip and vortex states. We set $t_{e0,\uparrow} = t_{h0,\uparrow} = t_{e1(2),\downarrow} = t_{h-1(-2),\downarrow} = 0.7\Delta$, $t_{e1(2),\uparrow} = t_{h-1(-2),\uparrow} = t_{e0,\downarrow} = t_{h0,\downarrow} = nt_{e0,\uparrow}$. We find that when n=0, the STM tip only coupling with the spin up channel of MZM and the spin down channel of the excited states. In this case, the coupling between electron and hole is only from the MZM. In case of $n \neq 0$, the STM tip have coupling with the spin up channel of the excited states.

Then, the influence of excited states on the conductance will increase with increase of n.

Besides, with increase of the θ, the coupling between the spin up channel and spin down channel is strong. The spin down channel that is majority component of wave function may have more contribution of conductance. However, when $\theta = 180^o$, the energy broadening is too small to suppress the contribution of excited states.

References

[S1] Hu L H, Li C, Xu D H, Zhou Y and Zhang F C 2016 Phys. Rev. B **94**, 224501.

[S2] Sau J D, Tewari S, Lutchyn R M, Stanescu T D and Sarma S D 2010 Phys. Rev. B 82, 214509.

[S3] Xu J P, Wang M X, Liu Z L, Ge J F, Yang X J, Liu C H, Xu Z A, Guan D D, Gao C L, Qian D, Liu Y, Wang Q H, Zhang F C, Xue Q K and Jia J F, 2015 Phys. Rev. Lett. 114, 017001,

[S4] Sergueev N, Sun Q F, Guo H, Wang B and Wang J 2002 Phys. Rev. B 65, 165303.

[S5] Fisher D S and Lee P A 1981 Phys. Rev. B 23, 6851.

[S6] Datta S Electronic Transport in Mesoscopic Systems, Cambridge Studies in Semiconductor Physics and Microelectronic Engineering (Cambridge University Press, Cambridge, 1997).

[S7] Blanter Y and Bttiker M 2000 Physics Reports 336, 1, ISSN 0370-1573,

[S8] He J J, Ng T K, Lee P A and Law K T 2014 Phys. Rev. Lett. 112, 037001.